

Identifying Topological Order by Entanglement Entropy

Hong-Chen Jiang^{1,2}, Zhenghan Wang³, and Leon Balents^{1,*}

¹Kavli Institute for Theoretical Physics, University of California, Santa Barbara, CA, 93106, U.S.A.

²Center for Quantum Information, IIS, Tsinghua University, Beijing, 100084, China

³Microsoft Station Q, University of California, Santa Barbara, CA, 93106, U.S.A.

*To whom correspondence should be addressed; E-mail: balents@kitp.ucsb.edu.

Topological phases are unique states of matter incorporating long-range quantum entanglement, hosting exotic excitations with fractional quantum statistics. We report a practical method to identify topological phases in arbitrary realistic models by accurately calculating the Topological Entanglement Entropy (TEE) using the Density Matrix Renormalization Group (DMRG). We argue that the DMRG algorithm naturally produces a minimally entangled state, from amongst the quasi-degenerate ground states in a topological phase. This proposal both explains the success of this method, and the absence of ground state degeneracy found in prior DMRG sightings of topological phases. We demonstrate the effectiveness of the calculational procedure by obtaining the TEE for several microscopic models, with an accuracy of order 10^{-3} when the circumference of the cylinder is around ten times the correlation length. As an example, we definitively show the ground state of the quantum $S = 1/2$ antiferromagnet on the kagomé lattice is a topological spin liquid, and strongly constrain the full identification of this phase of matter.

Theory has shown that quantum ground states may exhibit distinct patterns of *long-range entanglement*, which provides the most basic categorization of quantum phases of matter, more fundamental than Landau’s symmetry breaking paradigm. The simplest and most robust long range entangled states, which have a full spectral gap, comprise “topological phases”, which host topological order. Much recent interest in topological phases is due to the prospect of utilizing them to construct an inherently fault tolerant quantum computer (1, 2). Topological phases are also of basic scientific interest for their many unique properties, especially their ability to support exotic excitations with fractional and even non-abelian quantum statistics.

Crystalline “Mott” insulators with unpaired electron spins have long been considered likely candidates for long range entangled states, epitomized in this context by Anderson’s resonating valence bond (3) wavefunction for a “quantum spin liquid” (4). Because this particular state is non-magnetic, the lack of magnetic order has been widely taken as a definition of a quantum spin liquid. However, defining what a quantum spin liquid *isn’t* has little utility, and is especially unhelpful in the theoretical search for these phases. Instead, a *positive* definition of a quantum spin liquid which can be tractably tested in realistic models is sorely needed.

In principle, such a positive definition is provided for topological phases (and hence those quantum spin liquids with topological order) by the Topological Entanglement Entropy (TEE) introduced by Kitaev-Preskill (5) and Levin-Wen (6). Unfortunately, the formulations in Refs. (5, 6) suffer from severe finite-size corrections due to lattice scale effects, greatly hindering their application. We report here a practical and extremely simple scheme to numerically calculate the TEE, and thereby identify topological order. Our method consists simply of using the Density Matrix Renormalization Group (7, 8) (DMRG) to calculate the usual entanglement entropy for the division of a cylinder into two equal halves by a flat cut, and extracting the TEE from its asymptotic, large circumference limit (see below). We argue that this method actually works, despite potential complications known theoretically, (9, 10) due to a subtle ground state

selection mechanism built into the DMRG algorithm. The approach is tested here on a variety of lattice models, and then applied successfully to the physically realistic quantum spin $S = \frac{1}{2}$ anti-ferromagnetic Heisenberg J_1 - J_2 model on the kagomé lattice. By extracting an accurate TEE, we identify a quantum spin liquid state with topological order for the first time in a physically realistic $SU(2)$ -invariant lattice model. We emphasize that the TEE provides *positive*, “smoking gun” evidence for a topological quantum spin liquid, and excludes any topologically trivial states, regardless of possible complex or subtle broken symmetries. The *value* of the TEE also greatly restricts the possible topological quantum field theories which fully describe the topological order. We return to this at the end of this paper.

The TEE is derived from the bipartite von Neumann entanglement entropy, which is defined by dividing a system into two subsystems, A and B , which together comprise the full system. The entanglement entropy associated to this partition is defined from the reduced density matrix, $\rho_A = \text{Tr}(|0\rangle\langle 0|)$, where $|0\rangle$ is a ground state, according to $S(A) = -\text{Tr}[\rho_A \ln(\rho_A)]$. It has the duality property $S(A) = S(B)$. According to the seminal works of Kitaev-Preskill (5) and Levin-Wen (6), the entanglement entropy of a partition of a two dimensional system where A is a disk-like region with a *smooth* boundary (the “entanglement surface”) of length ℓ scales as

$$S(A) = \alpha\ell - \gamma + \dots, \tag{1}$$

where the ellipsis represents terms that vanish in the limit $\ell \rightarrow \infty$. The coefficient α , due to short distance physics near the boundary, is non-universal. The term γ is the topological entanglement entropy (TEE)—a universal additive constant characterizing the long-range entanglement in the ground state which can be quantified as $\gamma = \ln D$, where D is the total quantum dimension of the medium (5, 6).

Note that γ is *sub-dominant* to the $\alpha\ell$ term, arising from *short-range entanglement*. As a consequence, it is non-trivial to extract. Moreover, for real lattice systems, it is not obvious how

to define ℓ on the lattice, nor is it obvious what qualifies as a “smooth” boundary. These two ambiguities are particularly challenging.

In Refs. (5, 6), complex prescriptions were proposed to remove the short-range contributions and extract the TEE from measurements on planar partitions. In our much simpler scheme, we study a single partition, defined by a straight cut normal to a cylinder which divides it in half, and extract the TEE using Eq. (1) with $\ell = L_y$, the circumference of the cylinder. This approach minimizes errors due to subtractions of many large numbers, and also minimizes finite size corrections due to short-range entanglement, as we now argue.

For the cylindrical case, we expect such finite size corrections to be of order $e^{-L_y/\xi}$. In the Kitaev-Preskill and Levin-Wen formulations, the corrections are much larger. There, to obtain the TEE, the entropy is calculated for several disk-like planar partitions, and corner contributions are cancelled by forming a linear combination of the results. However, the complicated shape of the planar partitions involved means that the smallest spatial features of the partition are several times smaller than the overall system width. For instance, in the Levin-Wen formulation, the smallest features (size d) are *at least* four times smaller than the linear width of the system assuming periodic boundary conditions, so that $L \geq 4d$, a conservative estimate. Corrections to Eq. (1) should be expected to be of order $e^{-d/\xi} \geq e^{-L/(4\xi)}$. Thus to obtain similar performance to that of the cylindrical cut, even assuming no additional errors are introduced by the subtractions of different entropies, requires a *linear* system size at least four times larger in the Levin-Wen case. This means at least 16 times as many spins, and given the exponential growth of the Hilbert space with the number of quantum degrees of freedom, this is a very costly increase. Indeed, attempts to implement the Kitaev-Preskill and Levin-Wen protocols in simulations have shown them to be very challenging numerically (11, 12).

A potential complication of our method is that the ground state on a cylinder is expected to have a degeneracy in a topological phase in the thermodynamic limit, and the TEE for the cylin-

drical cut can depend upon *which* ground state the TEE is measured in (9, 10). In Ref. (10), it has been shown, however, that the TEE for the \mathbb{Z}_2 spin liquid is bounded above by the universal value $\gamma = \ln 2$, and below by zero. Moreover, in general the universal value is achieved for so-called Minimal Entropy States (MES's) (10), which correspond to states in which a quasi-particle is definitely contained within the region A (or B). For the \mathbb{Z}_2 spin liquid, the MES's are the states with a *definite* \mathbb{Z}_2 magnetic flux through the cylinder, i.e. the vison or no-vison eigenstates.

We suggest, based on numerical evidence, that *the DMRG systematically finds a MES*. This is perhaps natural since the DMRG prefers low entanglement states (8). Note though that the *absolute* ground state of a finite system is dependent upon microscopic details, and is expected to vary with the aspect ratio (L_x/L_y) of the cylinder (13). For a physical Hamiltonian without fine tuning, the absolute ground state becomes a MES in the “long” cylinder limit, where L_x/L_y is larger than some critical value (which depends on microscopic details, but is order one generically) (13). However, we contend that the DMRG preferentially finds the MES even when it is not the absolute ground state. Evidence for this is given below in the toric code model, where the MES can be explicitly identified. The fact that we obtain the universal value of the TEE, independent of the system's aspect ratio, for several other models, also supports this conclusion.

We turn now to the toric code model, which is well known – see the Supplementary material for details of the definition. It can be considered as a model of fluctuating discrete “electric” and “magnetic” fields. To observe the ground state selection, we first consider an applied field $h = h_x \neq 0$ which is purely electric, $h_z = 0$. Then the operator G (defined in the Supp. Mat.), which measures the parity of the number of electric field loops winding around the cylinder, commutes with the Hamiltonian, so the energy eigenstates must also be eigenstates of $G = \pm 1$. Topological order implies that there are two such states with $G = +1$ and $G = -1$, with

exponentially close energies. The MES's, however, are not G (or energy) eigenstates, but rather the superpositions $|\pm\rangle = (|G = 1\rangle \pm |G = -1\rangle)/\sqrt{2}$, for which $\langle \pm | G | \pm \rangle = 0$. The $|\pm\rangle$ states correspond to states with or without magnetic flux through the cylinder. Measurements of $\langle G \rangle$ and S , Figure 1, show that the DMRG preferentially selects a MES for larger systems, and that the number of states m necessary to converge to the absolute ground state (with larger entanglement and zero TEE – see Figure 2b) grows very rapidly with system size.

The origin of the topological contributions to the entanglement entropy sheds light on this behavior in the \mathbb{Z}_2 case of interest. First, there is a *reduction* of entropy due to the constraint that electric field loops always cross the entanglement surface an even number of times. This reduction is precisely the TEE, and this physics is included once entanglement on the scale of L_y is taken into account. Second, in the case where the absolute ground state is not a MES, there is an *increase* of entropy due to the *global* constraint on the number of electric field lines winding the *entire* cylinder. To take this into account, the DMRG must fully converge the entanglement of the opposite ends of the system, which are extremely far separated on the “snaking” DMRG path. This global entanglement does not converge for larger systems, in which case the DMRG produces states described by a Schmidt decomposition in which the left and right halves of the system have *uncorrelated* electric field winding parities. Such a state is a MES.

We next consider the toric code model in symmetrically applied fields, $h_x = h_z = h$, for which the absolute ground state is not obvious. Figure 2 shows the entanglement entropy in this case. This model was previously shown (14) to have a quantum phase transition between the \mathbb{Z}_2 phase for $h < h_c \approx 0.34$ and a trivial phase for $h > h_c$. The extrapolated TEE following our protocol indeed very well approximates the universal value $\gamma = \ln 2 = 0.69314\dots$ for $h < h_c$; even for $h = 0.3$, relatively close to the quantum phase transition, we obtain $\gamma = 0.691(4)$, which is accurate to a fraction of a percent. For $h > h_c$, we obtain $\gamma = 0$, as expected, with a numerical uncertainty of order 10^{-3} . Similar results are obtained for a variety of aspect ratios

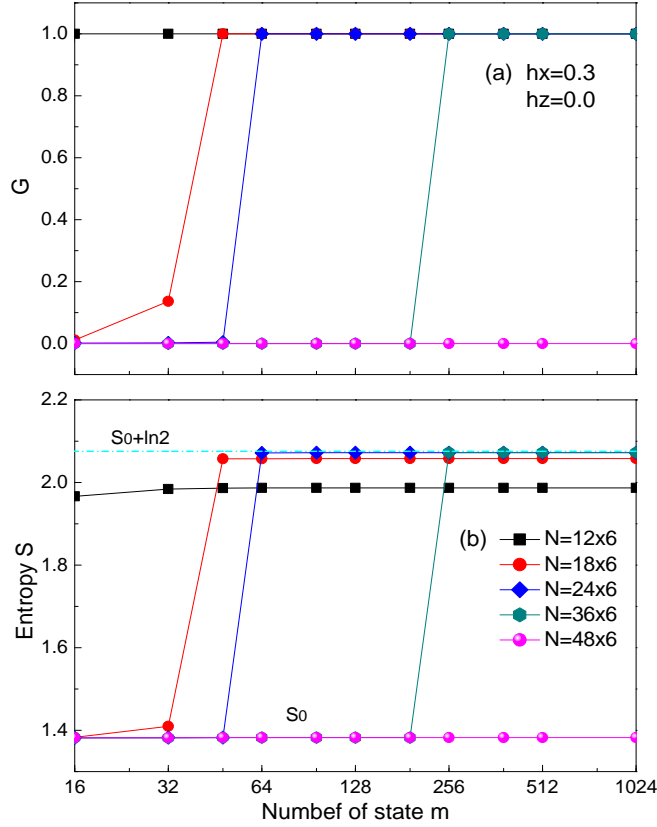


Figure 1: Evidence that the DMRG favors MES's. In (a) the electric field parity $\langle G \rangle$ and (b) the entanglement entropy are plotted versus number of states m for the toric code with $h_x = 0.3$ and $h_z = 0$, for several system sizes. We see that for fixed small system size, at smaller m the average parity $\langle G \rangle$ is approximately zero and the entanglement is reduced, while at large m a definite parity eigenstate is found with $G = 1$, and the entanglement is increased. The jumps in the two quantities coincide, signaling a transition from a MES to an absolute Hamiltonian eigenstate. The number of states m needed to converge to the absolute ground state increases rapidly with L_x . For larger systems than shown, a MES with $\langle G \rangle \approx 0$ is found for all accessible values of m .

and values of the perturbing fields.

We apply the method to the spin-1/2 Heisenberg model on the kagomé lattice, for which compelling but indirect evidence for a gapped quantum spin liquid has been recently obtained by extensive DMRG studies (15–17). We consider the model with both first and second-neighbor interactions, whose Hamiltonian is

$$H = J_1 \sum_{\langle ij \rangle} \mathbf{S}_i \cdot \mathbf{S}_j + J_2 \sum_{\langle\langle ij \rangle\rangle} \mathbf{S}_i \cdot \mathbf{S}_j, \quad (2)$$

where \mathbf{S}_i is the spin operator on site i , and $\langle ij \rangle$ ($\langle\langle ij \rangle\rangle$) denotes the nearest neighbors (next nearest neighbors). In the numerical simulation, we set $J_1 = 1$ as the unit of energy. The most recent DMRG studies (17) show that the $J_2 = 0$ point is near the edge of a substantial spin liquid phase centered near $J_2 = 0.05 - 0.15$.

We take the kagomé lattice with periodic boundary conditions along a bond direction, drawn vertically in the inset of Figure 3, and the unit of length equal to the nearest-neighbor distance. The results for the entanglement entropy for $J_2 = 0.10$ and 0.15 are shown in Figure 3 with correlation length around one-lattice spacing for both spin-spin and dimer-dimer correlation functions. We see that a linear fit using data for $L_y = 4 \sim 12$ using Eq.(1) gives $\gamma = 0.698(8)$ at $J_2 = 0.10$ and $\gamma = 0.694(6)$ at $J_2 = 0.15$, both within one percent of $\ln 2 = 0.693$. This proves definitively that this phase is a topological spin liquid, and determines the quantum dimension $D = 2$, very consistent with a \mathbb{Z}_2 state.

We have shown that the TEE can be calculated to an accuracy of order 10^{-3} when L_y is ~ 10 times the correlation length (see the Supporting Online Material for some additional tests). Our result provides a “smoking gun” test for a topological spin liquid. It also explains the puzzling absence of topological degeneracy in recent DMRG results which otherwise support a \mathbb{Z}_2 spin liquid state (13, 16), since we have shown that the DMRG is systematically biased to find just *one* of the ground states. The TEE does not fully determine the nature of the topological

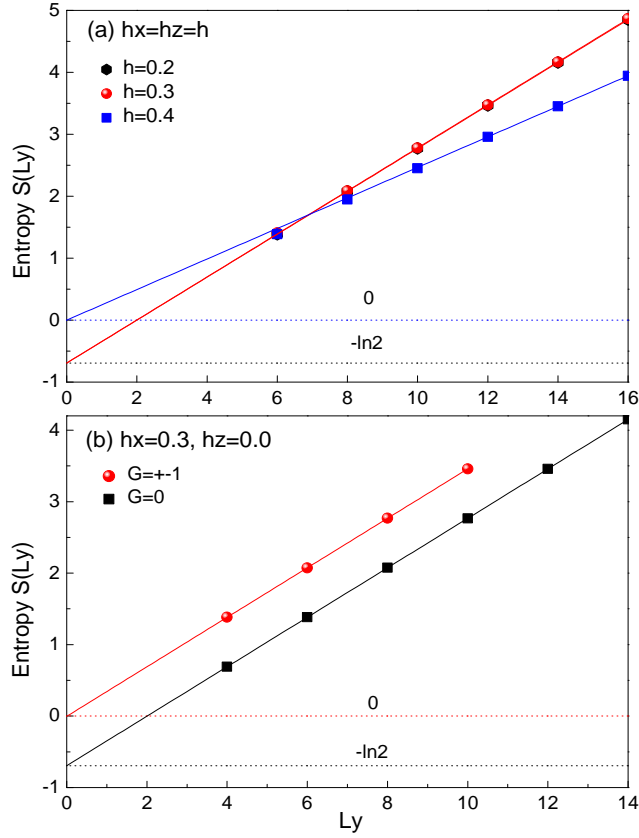


Figure 2: The von Neumann entropy $S(L_y)$ for the toric code model in magnetic fields. In (a), we show $S(L_y)$ with $L_y = 4 \sim 16$ at $L_x = \infty$ for symmetric magnetic fields at $h_x = h_z = h = 0.2, 0.3$ and 0.4 . By fitting $S(L_y) = aL_y - \gamma$, we get $\gamma = 0.693(1), 0.691(4)$ and $0.001(5)$, respectively. In (b), we consider the pure electric case, $h_x = 0.3, h_z = 0$, and compare $S(L_y)$ in the MES obtained in the large L_x limit (black squares) to that of the absolute ground state from systems of dimensions $L_x \times L_y = 20 \times 4, 24 \times 6, 24 \times 8, 24 \times 10$ (red circles). Extrapolation shows that the MES has the universal TEE, while the absolute ground state has zero TEE.

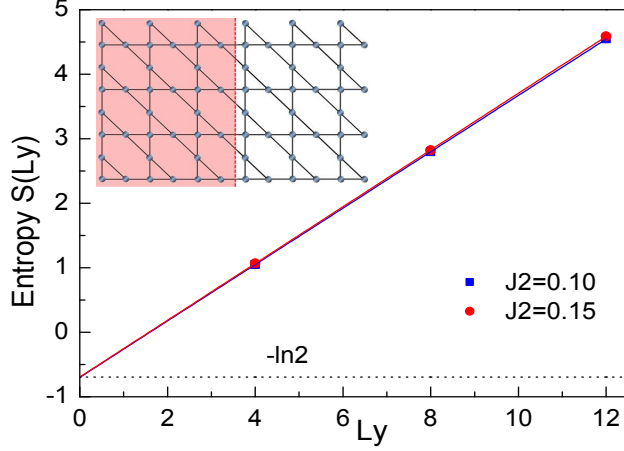


Figure 3: The entanglement entropy $S(L_y)$ of the kagomé J_1 - J_2 model in Eq.(2), with $L_y = 4 \sim 12$ at $L_x = \infty$. By fitting $S(L_y) = aL_y - \gamma$, we get $\gamma = 0.698(8)$ at $J_2 = 0.10$, and $\gamma = 0.694(6)$ at $J_2 = 0.15$. Inset: kagomé lattice with $L_x = 12$ and $L_y = 8$.

phase. Fortunately, for a given D , there are only finitely many distinct topological phases, and for small values of D , a complete classification of all topological phases is known (18). Other constraints such as time-reversal symmetry (if present) further constrain the possible topological order. For example, there are only two time-reversal invariant phases consistent with $D = 2$, found here for the kagomé Heisenberg model: the \mathbb{Z}_2 phase, and a doubled semion phase. It will be interesting to develop methods to distinguish these in the future, and to calculate the topological ground state splitting. Identifying topological order by combining theoretical classification results with numerical simulation is a major step in the development of a post-Landau paradigm for classifying quantum phases of matter.

References and Notes

1. A. Y. Kitaev, Fault-tolerant quantum computation by anyons, *Ann. Phys. (N.Y.)* **303**, 2 (2003).
2. C. Nayak, S. H. Simon, A. Stern, M. Freedman, S. Das Sarma, Non-abelian anyons and

- topological quantum computation, *Rev. Mod. Phys.* **80**, 1083 (2008).
3. P. W. Anderson, Resonating valence bonds: a new kind of insulator?, *Materials Research Bulletin* **8**, 153 (1973).
 4. L. Balents, Spin liquids in frustrated magnets, *Nature* **464**, 199 (2010).
 5. A. Kitaev, J. Preskill, Topological entanglement entropy, *Phys. Rev. Lett.* **96**, 110404 (2006).
 6. M. Levin, X.-G. Wen, Detecting topological order in a ground state wave function, *Phys. Rev. Lett.* **96**, 110405 (2006).
 7. S. R. White, Density matrix formulation for quantum renormalization groups, *Phys. Rev. Lett.* **69**, 2863 (1992).
 8. E. M. Stoudenmire, S. R. White, Studying two dimensional systems with the density matrix renormalization group, *arXiv:1105.1374* (2011).
 9. S. Dong, E. Fradkin, R. G. Leigh, S. Nowling, Topological entanglement entropy in Chern-Simons theories and quantum Hall fluids, *JHEP* **0805**, 016 (2008).
 10. Y. Zhang, T. Grover, A. Turner, M. Oshikawa, A. Vishwanath, Quasi-particle statistics and braiding from ground state entanglement, *arXiv:1111.2342* (2011).
 11. S. Furukawa, G. Misguich, Topological entanglement entropy in the quantum dimer model on the triangular lattice, *Phys. Rev. B* **75**, 214407 (2007).
 12. S. V. Isakov, M. B. Hastings, R. G. Melko, Topological entanglement entropy of a bose-hubbard spin liquid, *Nature Physics* **7**, 772 (2011).

13. H. C. Jiang, H. Yao, L. Balents, Spin liquid ground state of the spin-1/2 square J_1 - J_2 Heisenberg model, *arXiv:1112.2241* (2011).
14. S. Trebst, P. Werner, M. Troyer, K. Shtengel, C. Nayak, Breakdown of a topological phase: Quantum phase transition in a loop gas model with tension, *Phys. Rev. Lett.* **98**, 070602 (2007).
15. H. C. Jiang, Z. Y. Weng, D. N. Sheng, Density matrix renormalization group numerical study of the kagome antiferromagnet, *Phys. Rev. Lett.* **101**, 117203 (2008).
16. S. Yan, D. Huse, S. White, Spin-liquid ground state of the $s=1/2$ kagome heisenberg antiferromagnet, *Science* **332**, 1173 (2011).
17. S. R. White, The spin liquid ground state of the $S=1/2$ Heisenberg model on the kagome lattice, *March Meeting 2012, Invited talk in session L19, 1 at <http://meetings.aps.org/link/BAPS.2012.MAR.L19.1>* (2012).
18. E. Rowell, R. Stong, Z. Wang, On classification of modular tensor categories, *Comm. Math. Phys.* **292**, 343 (2009).
19. J. Vidal, S. Dusuel, K. P. Schmidt, Low-energy effective theory of the toric code model in a parallel magnetic field, *Phys. Rev. B* **79**, 033109 (2009).
20. I. S. Tupitsyn, A. Kitaev, N. V. Prokof'ev, P. C. E. Stamp, Topological multicritical point in the phase diagram of the toric code model and three-dimensional lattice gauge higgs model, *Phys. Rev. B* **82**, 085114 (2010).
21. F. D. M. Haldane, Model for a quantum hall effect without landau levels: Condensed-matter realization of the "parity anomaly", *Phys. Rev. Lett.* **61**, 2015 (1988).

22. Y.-F. Wang, Z.-C. Gu, C.-D. Gong, D. N. Sheng, Fractional quantum hall effect of hard-core bosons in topological flat bands, *Phys. Rev. Lett.* **107**, 146803 (2011).
23. H. W. J. Blöte, Y. Deng, Cluster monte carlo simulation of the transverse ising model, *Phys. Rev. E* **66**, 066110 (2002).
24. M. P. Gelfand, R. R. P. Singh, D. A. Huse, Zero-temperature ordering in two-dimensional frustrated quantum heisenberg antiferromagnets, *Phys. Rev. B* **40**, 10801 (1989).
25. S. Sachdev, Quantum phase transitions of antiferromagnets and the cuprate superconductors, *arXiv:1002.3823* (2010).
26. We thank Tarun Grover and Ashvin Vishwanath for a helpful explanation of their work, and Steve White for helpful discussions. H.C.J. thanks Hong Yao for collaboration on related projects. This work was supported by the NSF through grant DMR=0804564 (L.B.), the NSF MRSEC Program under DMR 1121053, the NBRPC (973 Program) 2011CBA00300 (2011CBA00302), and benefitted from the facilities of the KITP, supported by NSF PHY05-51164.

26. **Supporting Online Material**

www.sciencemag.org

Materials and Methods

Figures S1, S2, S3

References (19-25)

Supporting Online Material

Materials and Methods

Here we test our method on a variety of lattice models whose topological order is known.

A Toric-code model in magnetic fields

The toric code model (I) with an applied magnetic field is given by

$$H = -J_s \sum_s A_s - J_p \sum_p B_p - h_x \sum_i \sigma_i^x - h_z \sum_i \sigma_i^z, \quad (\text{S1})$$

where σ_i^x and σ_i^z are Pauli matrices, and $A_s = \prod_{i \in s} \sigma_i^x$, $B_p = \prod_{i \in p} \sigma_i^z$. Subscripts s and p refer to, respectively, vertices and plaquettes of a square lattice, whereas i runs over all bonds where spin degrees of freedom are located. Without magnetic field, i.e., $h_x = h_z = 0$, the pure toric code model can be solved exactly (I), and the ground state has \mathbb{Z}_2 topological order with total quantum dimension $D = 2$. On the torus the ground state is 4-fold degenerate. All elementary excitations are gapped and characterized by eigenvalues $A_s = -1$ (a \mathbb{Z}_2 charge on site s) and $B_p = -1$ (a \mathbb{Z}_2 vortex on plaquette p). When turning on the magnetic field, the model cannot be solved exactly anymore. Previous studies (*14, 19, 20*) show that the \mathbb{Z}_2 topological phase remains stable and robust until the magnetic fields are large enough, where the system crosses the transition from the topological phase to the trivial one. Specifically, such a phase transition takes place at the critical magnetic field $h_c = 0.34$ along the symmetric line $h_x = h_z = h$.

For the DMRG simulation, we consider an equivalent square lattice, where the spin operators σ^x and σ^z sit on the sites instead of the bonds. Therefore, the star operator A_s and the plaquette operator B_p of the original lattice now sit on alternating plaquettes in the equivalent square lattice, as shown in Figure S1, labeled as S and P , respectively. Note that on this equivalent square lattice, there are an even number of dangling spins within each plaquette at the

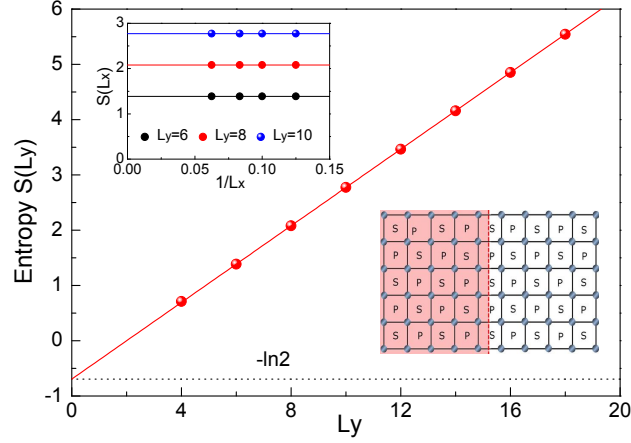


Figure S1: The von Neumann entropy for the pure toric code model and that in magnetic fields in Eq.(S1). The von Neumann entropy $S(L_y)$ for the pure Toric-Code model with $L_y = 4 \sim 20$ at $L_x = \infty$. By fitting $S(L_y) = aL_y - \gamma$, we get $\gamma = 0.693147(1)$. Inset: (Upper) the entanglement entropy $S(L_x)$ as a function of L_x for different L_y ; and (Lower) Square lattice with $L_x = 10$ and $L_y = 6$. Here S represents the star operator A_s , while P represents the plaquette operator B_p .

open edges. For the pure toric-code model with cylinder boundary condition, the first $2^{L_y/2-1}$ eigenvalues of the reduced density matrix ρ_A are degenerate and equal to $1/2^{L_y/2-1}$, while all the other eigenvalues are zero. This allows us to study a quite large system with width up to $L_y = 20$ easily. As shown in Figure S1, after fitting the entanglement entropy using Eq.(1) for $L_x = \infty$, we get a nonzero topological entanglement entropy $\gamma = 0.693147(1)$, which is equal to the expected value $\gamma = \ln 2$ with amazingly small numerical error 10^{-6} .

After turning on the magnetic field, the degeneracy of entanglement spectrum is lifted, and the correlation length ξ becomes finite. Our results show that even very close to the phase transition point (e.g., $h_c = 0.34$ along the symmetric line), we can still get a very accurate TEE γ . For example, the correlation length $\xi \sim 1$ lattice spacing at $h = 0.30$, the resulted topological entanglement entropy $\gamma = 0.691(4)$ is still quite accurate with an error around 10^{-3} . These results show that a nonzero TEE is obtained throughout the topologically ordered phase. On the contrary, the topological entanglement entropy γ is zero in the trivial phase where $h > h_c$.

For example, $\gamma = 0.001(5)$ at $h = 0.40$. Therefore, our method allows us to unambiguously extract the non-zero topological entanglement entropy γ if and only if the toric-code model is in a topologically ordered phase.

In the case of a purely electric perturbation, $h_z = 0$, $h_x = h \neq 0$, two loop operators commute with H . Specifically, these are

$$G = G_y = \prod_{x=1}^{L_x} \sigma_{x,y}^x, \quad (\text{S2})$$

$$G_x = \prod_{y=1}^{L_y} \sigma_{x,y}^x. \quad (\text{S3})$$

In the low energy sector where $A_s = +1$ for all s , G_y is independent of y and G_x is independent of x . By construction, G and G_x have eigenvalues ± 1 . The operator G_x probes the presence or absence of an electric particle at the end of the cylinder. This degree of freedom is not associated to the ground state degeneracy, and indeed we find $G_x = +1$ always in our numerics. The operator G counts the parity of the number of electric flux lines winding around the cylinder, and *does* operate in the topologically degenerate subspace. Physically, eigenstates of G are equal weight superpositions of the vison and no-vison eigenstates, which are the MES, as discussed in the main text. For $h_z = 0$, the energy eigenstates must also be eigenstates of G , and the splitting between them is expected to be exponentially small in L_x .

B Fractional quantum Hall model

We next consider the so-called Haldane model (21) on the honeycomb lattice filled with hardcore bosons:

$$\begin{aligned} H = & -t' \sum_{\langle\langle rr' \rangle\rangle} \left[b_{r'}^\dagger b_r e^{i\phi_{r'r}} + \text{H.c.} \right] \\ & - t \sum_{\langle rr' \rangle} \left[b_{r'}^\dagger b_r + \text{H.c.} \right] - t'' \sum_{\langle\langle\langle rr' \rangle\rangle\rangle} \left[b_{r'}^\dagger b_r + \text{H.c.} \right], \end{aligned} \quad (\text{S4})$$

where b_r^\dagger creates a hard-core boson at site r , $\langle \dots \rangle$, $\langle\langle \dots \rangle\rangle$, and $\langle\langle\langle \dots \rangle\rangle\rangle$ denote the nearest-neighbor, the next-nearest-neighbor, and the next-next-nearest-neighbor pairs of sites, respectively. In Ref. (22), the authors have systematically studied this model using exact diagonalization, providing convincing evidence showing that the ground state (with parameters $t' = 0.6t$, $t'' = -0.58t$, and $\phi = 0.4\pi$) is a $1/2$ bosonic FQH state with two-fold ground state degeneracy on the torus. Such a $1/2$ FQH state has nontrivial semion topological order $(5, 6)$, with total quantum dimension $D = \sqrt{2}$.

For the numerical simulation, we consider a honeycomb lattice with length vectors $L_1\mathbf{a}_1$ and $L_2\mathbf{a}_2$ as shown in the inset (a) of Figure S2. Here $\mathbf{a}_1 = (\sqrt{3}, 0)$ and $\mathbf{a}_2 = (\frac{\sqrt{3}}{2}, \frac{3}{2})$ are two primitive vectors of the unit cell which includes two sites of the lattice. The total number of sites is $N = 2 \times L_1 \times L_2$, with $L_1 \times L_2$ unit cells. Note that the corresponding system width $L_y = 2L_2$, and system length $L_x = 2L_1$. Unambiguously, extrapolation from the data for $L_y \leq 20$ using Eq.(1) shows that we can get a nonzero constant topological entanglement entropy $\gamma = 0.349(5)$. This is equal to $\ln(\sqrt{2}) = 0.347$ within the numerical error, showing that our method can also be used to study chiral topological states as well.

C Transverse-field Ising model

The models studied above have topologically ordered ground states, for which our method indeed gives us non-zero topological entanglement entropy with high accuracy. Now, we show that for a topologically trivial phase, our method unambiguously gives zero topological entanglement entropy as well. To show this, consider the well-known transverse field quantum Ising model

$$H = - \sum_{\langle ij \rangle} \sigma_i^z \sigma_j^z - h \sum_i \sigma_i^x, \quad (\text{S5})$$

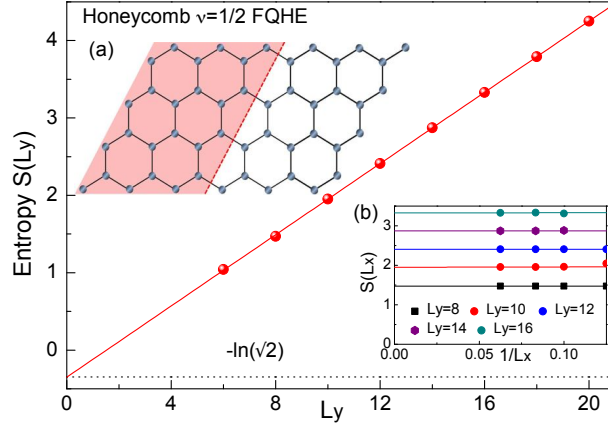


Figure S2: The entanglement entropy $S(L_y)$ of the Honeycomb Haldane model in Eq.(S5), with $L_y = 6 \sim 20$ at $L_x = \infty$. By fitting $S(L_y) = aL_y - \gamma$, we get $\gamma = 0.349(5)$. Inset: (a) Honeycomb lattice with $L_1 = 6$ and $L_2 = 4$. Here the system width $L_y = 2L_2$, and system length $L_x = 2L_1$. (b) The entanglement entropy $S(L_x)$ as a function of L_x for different L_y .

where σ_i^x and σ_i^z are Pauli matrices on site i . This model is known to have a topological trivial ground state in all magnetic fields, and a second order phase transition at critical field $h_c = 3.044$ (23). As shown in Figure S3(a), our method produces very accurate results showing $\gamma = 0$ even very close to the phase transition point. For example, at $h = 3.1$, we obtain $\gamma = 0.0014(5)$, which is zero within the numerical error, despite the longish correlation length $\xi \sim 4$ for $\langle S^z S^z \rangle$ and $\xi \sim 1$ for $\langle S^x S^x \rangle$ in this case.

D Coupled spin-dimer model

Another well-known model with a topologically trivial ground state is the coupled spin-dimer model,

$$H = \sum_{\langle ij \rangle \in A} \mathbf{S}_i \cdot \mathbf{S}_j + g \sum_{\langle ij \rangle \in B} \mathbf{S}_i \cdot \mathbf{S}_j, \quad (\text{S6})$$

where \mathbf{S}_i is the spin- $\frac{1}{2}$ operator on site i on the square lattice shown in the inset of Figure S3(b), with A links forming decoupled dimers while B links couple the dimers. The ground state of

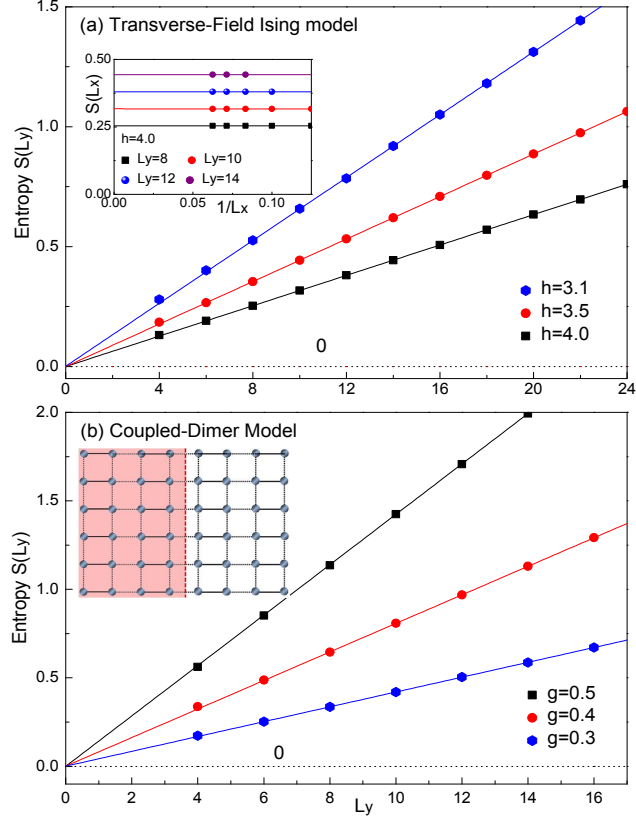


Figure S3: The entanglement entropy of the transverse field quantum Ising model and coupled spin-dimer model. (a) The entanglement entropy $S(L_y)$ of the transverse field quantum Ising model in Eq.(S5) with $L_y = 4 \sim 24$ at $L_x = \infty$, in different magnetic field $h = 3.1, 3.5$ and 4.0 . By fitting $S(L_y) = aL_y - \gamma$, we get $\gamma = 0.0014(5), 0.0004(4)$ and $0.0001(2)$, respectively. Inset: The entanglement entropy $S(L_x)$ as a function of L_x for different L_y at $h = 4.0$. (b) The entanglement entropy $S(L_y)$ of the coupled spin-dimer model in Eq.(S6) with $L_y = 4 \sim 16$ at $L_x = \infty$, at different coupling $g = 0.5, 0.4$ and 0.3 . By fitting $S(L_y) = aL_y - \gamma$, we get $\gamma = 0.006(6), 0.002(1)$ and $0.0008(9)$, respectively. Inset: The coupled spin-dimer model, with spin ($S = \frac{1}{2}$) on the sites, the A links are shown as full lines, and the B links as dashed lines.

Eq.(S6) depends only on the dimensionless coupling g . It is known that there is an gapped dimerized phase for $g < g_c = 0.52$ (24, 25), at which point a second order phase transition occurs. Unlike in the transverse field quantum Ising model in Eq.(S5), spin rotational symmetry is preserved in this model, although the lattice translational symmetry is explicitly broken. Unambiguously, as shown in Figure S3(b), our method once more produces very accurate results showing $\gamma = 0$ even quite close to the phase transition point. For example, $\gamma = 0.006(6)$ at $g = 0.50$, which is zero within the numerical error.